

International Journal of Modern Physics A  
© World Scientific Publishing Company

## ALPHA CLUSTERING AND WEAK COUPLING IN THE $^{93}\text{Nb}$ REGION

S. Ohkubo\*

*Department of Applied Science, Kochi Women's University, Kochi 780-8515, Japan and  
Research Center for Nuclear Physics, Osaka University, Ibaraki, Osaka 567-0047, Japan*

Received October 14, 2018

From the viewpoint of a unified description of cluster structure and scattering in the  $A = 90$  region,  $\alpha$  scattering from  $^{89}\text{Y}$  is investigated.  $\alpha$  clustering and weak coupling in  $^{93}\text{Nb}$  is discussed.

*Keywords:*  $\alpha$  clustering in  $^{93}\text{Nb}$ ;  $\alpha+^{89}\text{Y}$  scattering; weak coupling.

PACS numbers: 21.60.Gx, 24.10.Ht, 25.55.Ci, 27.60.+j

### 1. Introduction

It has been widely accepted that the  $\alpha$  cluster structure exists in light nuclei.<sup>1,2</sup> It has been also shown that the  $\alpha$  cluster picture persists even in the  $fp$ -shell region like  $^{44}\text{Ti}$  where the spin-orbit force becomes strong.<sup>3-5</sup>

Clustering is realized due to the logic that the interaction of subunit clusters in nuclei is *internally (intracluster) strong but externally (intercluster) weak*.<sup>1</sup> This is most typically seen in  $^8\text{Be}$  with the  $\alpha+\alpha$  cluster structure. This logic of *internally strong but externally weak* is justified by a microscopic model study which uses a two-body nuclear force and fully takes into account the Pauli principle.<sup>1</sup>

In the  $p$ -shell closure region,  $^{16}\text{O} \sim ^{20}\text{Ne}$ , a weak coupling model was proposed phenomenologically<sup>6</sup> to account for the similarity of the structure of the rotational band built on the mysterious  $0^+$  state of  $^{16}\text{O}$  at 6.06 MeV and the intruder band in  $^{19}\text{F}$  starting from the  $\frac{1}{2}^-$  state at 0.11 MeV to the ground band of  $^{20}\text{Ne}$ . Nemoto and Bandō<sup>7</sup> clarified in the microscopic model that this weak coupling is a consequence of both the development of  $\alpha$  clustering and the Pauli principle, which causes internally strong and externally weak binding of the clusters.

The persistency of this weak coupling due to  $\alpha$  clustering in the  $sd$ -shell closure region,  $^{40}\text{Ca} \sim ^{44}\text{Ti}$ , was also shown.<sup>5</sup> It is important to know whether this weak coupling is universal and persists in much heavier nuclei where the closed shells for

\*shigeo@cc.kochi-wu.ac.jp

2 *S. Ohkubo*

protons and neutrons are different. It is the purpose of this paper to study whether the weak coupling picture due to  $\alpha$  clustering still persists in the  $A = 90$  region.

## 2. $\alpha$ clustering in the $A = 90$ region

The structure of nuclei in the  $A = 90$  region has been mostly studied in the shell model and many properties have been successfully explained.<sup>8–10</sup> However, for some nuclei the existence of intruder states, which are difficult in the shell model, have been suggested. For example, in the typical nucleus  $^{94}\text{Mo}$ , which has two protons and two neutrons outside the double closed shell, the shell model calculation needs a large effective charge to explain the large  $B(E2)$  values of the ground band.

On the other hand, from the viewpoint of a unified description of bound and scattering for the  $\alpha + ^{90}\text{Zr}$  system, the present author suggested that the  $\alpha$  cluster model is still successful in understanding the structure of  $^{94}\text{Mo}$ .<sup>11</sup> The structure of  $^{94}\text{Mo}$  is also described in the  $\alpha + ^{90}\text{Zr}$  cluster model using a phenomenological potential<sup>12–15</sup> and a double folding model potential.<sup>13</sup>

Although there are not many experimental data of  $\alpha$  transfer reactions in this region compared with the  $^{20}\text{Ne}$  and  $^{44}\text{Ti}$  regions, there are some indications which suggest the importance of  $\alpha$  clustering in this mass region. For example, Molnár *et al.*<sup>16</sup> suggested that the intruder band states  $0^+$  (1.581 MeV),  $2^+$  (2.225 MeV) and  $4^+$  (2.857 MeV) in  $^{96}\text{Zr}$  have four-particle four-hole character just as in  $^{16}\text{O}$ . In the  $^{90}\text{Zr} \sim ^{94}\text{Mo}$  region  $\alpha$  transfer reactions, which were very powerful in light nuclei in selectively populating the  $\alpha$  cluster states, were reported.<sup>4, 17–20</sup> However, the  $\alpha$  cluster states have not been clearly identified. Therefore another approach from the viewpoint of  $\alpha$  clustering seems necessary.

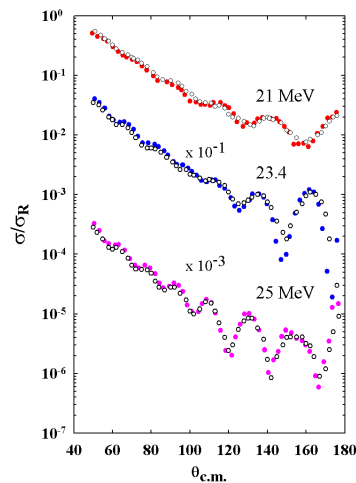


Fig. 1. (Color online) The similarity of the experimental angular distributions of  $\alpha + ^{89}\text{Y}$  (filled circles) and  $\alpha + ^{90}\text{Zr}$  scattering (open circles) at  $E_\alpha = 21, 23.4$  and  $25$  MeV<sup>21</sup> is shown.

A unified description of  $\alpha$  cluster bound states and  $\alpha$  particle scattering may be one of the useful approaches in this region. In fact, in the  $^{44}\text{Ti}$  region where  $\alpha$  transfer reactions were not sufficiently available, a unified description of bound states and  $\alpha$  particle scattering from  $^{40}\text{Ca}$  using a global potential was powerful in revealing the  $\alpha$  clustering aspects in  $^{44}\text{Ti}$  and  $^{40}\text{Ca}$ .<sup>3</sup> Because the structure of the typical nucleus  $^{94}\text{Mo}$  has been shown to be described in the  $\alpha$  cluster model, it seems useful to take this approach for the nuclei in the  $^{90}\text{Zr}\sim^{94}\text{Mo}$  region. In fact, as displayed in Fig. 1, the observed angular distributions in  $\alpha$  particle scattering from  $^{89}\text{Y}$  at  $E_\alpha=21\text{-}25$  MeV are very similar to those for  $\alpha+^{90}\text{Zr}$  scattering. The observed excitation function at  $\theta_{\text{c.m.}}=176^\circ$  for  $\alpha+^{89}\text{Y}$  scattering shows a deep minimum at around  $E_\alpha=23.4$  MeV similar to that for  $\alpha+^{90}\text{Zr}$  scattering.<sup>21</sup> Furthermore, as seen in Fig. 2, the band structures built on the 4p-nh states resemble each other as was the case in the  $^{16}\text{O}\sim^{20}\text{Ne}$  region.<sup>7</sup>

The above two facts, the close angular distributions in the scattering (Fig. 1) and the energy levels with a similar band structure (Fig. 2), suggest that the potentials for the  $\alpha+^{89}\text{Y}$  and the  $\alpha+^{90}\text{Zr}$  systems are very similar. As the  $\alpha+^{90}\text{Zr}$  structure in  $^{94}\text{Mo}$  is an analog of the  $\alpha+^{16}\text{O}$  cluster structure in  $^{20}\text{Ne}$  and the  $\alpha+^{40}\text{Ca}$  cluster structure in  $^{44}\text{Ti}$ , the  $\alpha+^{89}\text{Y}$  structure in  $^{93}\text{Nb}$  may be regarded an analog of the  $\alpha+^{15}\text{N}$  structure in  $^{19}\text{F}$  in the  $sd$ -shell and the  $\alpha+^{39}\text{K}$  structure in  $^{43}\text{Sc}$  in the  $fp$ -shell. Therefore, to clarify whether the weak coupling feature persists in the heavier  $A=90$  region it seems useful to study the  $\alpha+^{89}\text{Y}$  cluster structure of  $^{93}\text{Nb}$  in comparison with the  $\alpha+^{90}\text{Zr}$  structure of  $^{94}\text{Mo}$ . Recently Kiss *et al.*<sup>24</sup> extended the measurement of  $\alpha+^{89}\text{Y}$  scattering to the lower energies,  $E_\alpha=16.2$  and 19.4 MeV.

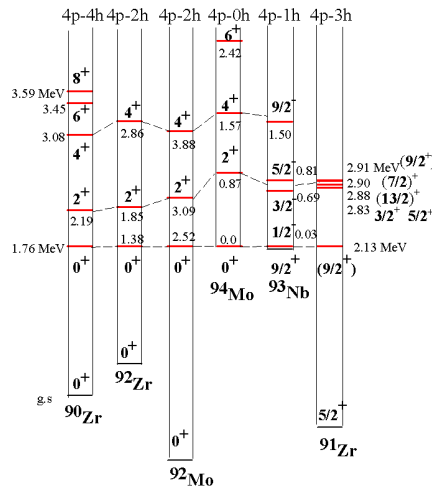


Fig. 2. (Color online) Experimental energy levels<sup>22, 23</sup> of the candidates for the  $\alpha$  cluster (4p-nh) states with the weak coupling feature in the  $^{90}\text{Zr}\sim^{94}\text{Mo}$  region are displayed connected by the dashed lines so that the band head states are in coincidence. Excitation energies are given in MeV.

4 *S. Ohkubo*

Also a large  $B(E2)$  value of the electric transition in  $^{93}\text{Nb}$  has been observed by Orce *et al.*<sup>23</sup>

### 3. Analysis of $\alpha$ particle scattering from $^{89}\text{Y}$

We analyze the  $\alpha+^{89}\text{Y}$  scattering by taking a Woods-Saxon squared phenomenological potential, which is similar to the one used for the  $\alpha+^{90}\text{Zr}$  system.<sup>11,14</sup> The form factor of the optical potential is given in the standard notation as follow:<sup>14</sup>

$$V(r) = -V_0\{1 + \alpha \exp[-(r/\rho)^2]\}/\{1 + \exp[(r - R_V)/2a_V]\}^2 + V_C(r), \quad (1)$$

$$W(r) = -W_0/\{1 + \exp[(r - R_W)/2a_W]\}^2, \quad (2)$$

for the real and imaginary potentials, respectively. The Coulomb potential  $V_C(r)$  is assumed to be a uniformly charged sphere with a radius  $R_c=7.49$  fm. The real potential parameters  $V_0=35$  MeV,  $R_V=7.49$  fm,  $a_V=0.43$  fm,  $\rho=4.86$  fm and  $\alpha=4.748$  are fixed for all the incident energies. The  $V_0$ ,  $a_V$  and  $\alpha$  parameters are the same as those for the  $\alpha+^{90}\text{Zr}$  system, and the  $R_V$  and  $\rho$  parameters are scaled from those for the  $\alpha+^{90}\text{Zr}$  system.<sup>14</sup> The imaginary potential parameters were adjusted to fit the data and are given in Table I.

As shown in Fig. 3, a good agreement is obtained with the experimental data. The characteristic deep minimum in the angular distribution at the extreme backward angle at  $E_\alpha=23.4$  MeV, which is also seen in the  $\alpha+^{90}\text{Zr}$  scattering (Fig. 1), is well reproduced by the calculation. As discussed in the  $\alpha+^{90}\text{Zr}$  scattering,<sup>14</sup> the

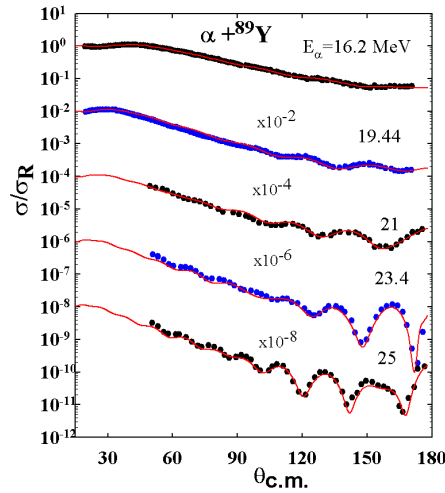


Fig. 3. (Color online) Calculated angular distributions in  $\alpha+^{89}\text{Y}$  scattering (solid lines) are compared with the experimental data (circles).<sup>21,24</sup>

oscillatory structure of the angular distribution at the backward angular region and the deep minimum at the extreme backward angle  $\theta_{\text{c.m.}}=176^\circ$  at  $E_\alpha=23.4$  MeV are caused by the interference between the internal waves, which penetrate deep into the internal region of the potential and the barrier waves, which are reflected at the surface region of the potential. This shows that absorption is incomplete and transparent for the  $\alpha+^{89}\text{Y}$  scattering in this energy region and the potential can be checked not only at the surface region but also in the internal region. This means that the real part of the obtained potential may be used for the  $\alpha+^{89}\text{Y}$  cluster structure calculation in  $^{93}\text{Nb}$ .

Table 1. Imaginary potential parameters used in the analysis of the angular distributions in  $\alpha + ^{89}\text{Y}$  scattering.

$E_\alpha$ (MeV)	$W_0$ (MeV)	$R_W$ (fm)	$a_W$ (fm)
16.2	14.5	7.04	0.162
19.44	11.6	7.71	0.135
21	16.1	6.47	0.08
23.4	17.0	6.44	0.135
25	17.6	6.44	0.135

#### 4. $\alpha$ clustering in $^{93}\text{Nb}$ and weak coupling

As shown in Fig. 4, in  $^{93}\text{Nb}$  the first excited state  $\frac{1}{2}^-$  appears at an extremely low excitation energy,  $E_x=0.031$  MeV above the ground state  $\frac{9}{2}^+$  similar to the  $\frac{1}{2}^-$  state at 0.11 MeV with a well-developed  $\alpha+^{15}\text{N}$  cluster structure in  $^{19}\text{F}$ . In the  $\alpha$  cluster model this state may be understood qualitatively that an  $\alpha$  particle is orbiting around the core nucleus  $^{89}\text{Y}(\frac{1}{2}^-)$  with an orbital angular momentum  $L = 0$ . The  $\frac{3}{2}^-$  state at  $E_x=0.687$  MeV and the  $\frac{5}{2}^-$  state at  $E_x=0.810$  MeV are considered to be doublet states, in which the  $\alpha$  particle is orbiting around the core with  $L = 2$ . Recently Orce *et al.*<sup>23</sup> observed a strong  $E2$  transition from the  $\frac{9}{2}^-$  state at  $E_x=1.500$  MeV to the  $\frac{5}{2}^-$  state ( $E_x=0.810$  MeV) with  $B(E2)=26.4_{-6.2}^{+9.7}$  W.u. This state may be considered to be a partner of the doublet states, in which the  $\alpha$  particle is coupled to the core with  $L = 4$ . The state at 1.364 MeV is reported to be  $\frac{5}{2}^-$  or  $\frac{7}{2}^-$ .<sup>22</sup>

The calculated energy levels and the  $B(E2)$  values are displayed in Fig. 4 in comparison with the experimental data.<sup>22,23</sup> In the calculation of the  $\alpha$  cluster structure we take the real potential parameters used in the analysis of  $\alpha + ^{89}\text{Y}$  scattering. To take account of the angular momentum dependence of the real potential, as discussed in Ref.[11], we assume  $\alpha=\alpha_0-cL$ .  $\alpha_0=4.17$  is fine tuned to reproduce the experimental threshold energy and  $c=0.005$  is used, which is very small, consistent with the values needed in the  $^{44}\text{Ti}$  and  $^{94}\text{Mo}$  cases.<sup>11</sup> No spin-orbit potential is introduced. The calculated  $N = 16$  band states, which satisfy the Wildermuth

6 *S. Ohkubo*

condition  $N=2n + L=16$  with  $n$  being the number of nodes of the relative wave function, fall well near the experimental states. The agreement of the calculated energy levels with the experimental data is good. The experimental  $B(E2)$  value of the  $E2$  transition from the  $\frac{9}{2}^-$  state (1.500 MeV) to the  $\frac{5}{2}^-$  state (0.810 MeV) is reproduced well with a small effective charge  $\delta e=0.2$ , which is consistent with the value in Ref.[11]. In Fig. 4, we note that the calculated and observed  $B(E2)$  values for  $^{93}\text{Nb}$  are comparable to the observed values for  $^{94}\text{Mo}$ . Thus it is found that the  $\alpha$  cluster model works in  $^{93}\text{Nb}$  in addition to  $^{94}\text{Mo}$  and the structure of the energy levels and the  $B(E2)$  values suggests that weak coupling picture due to  $\alpha$  clustering persists in this mass region. The  $\alpha$ -hole energy estimated from the experimental binding energies of  $^{94}\text{Mo}$ ,  $^{90}\text{Zr}$ ,  $^{93}\text{Nb}$ ,  $^{89}\text{Y}$  and the  $\alpha$  particles is 0.17 MeV for a proton hole in the  $2p_{\frac{1}{2}}$  shell. This is still small compared with 0.86 MeV of the  $\alpha$ -hole energy in  $^{19}\text{F}$ .<sup>6</sup> It is desired to observe the  $E2$  transition from the  $\frac{5}{2}^-$  state (0.810 MeV) to the  $\frac{1}{2}^-$  (0.031 MeV) and to compare with the predicted value.

### 5. Summary

We have studied  $\alpha+^{89}\text{Y}$  scattering and the  $\alpha+^{89}\text{Y}$  cluster structure in  $^{93}\text{Nb}$  in a unified way by using a phenomenological potential. It is found that the potential which reproduces the angular distributions in  $\alpha+^{89}\text{Y}$  scattering is very similar to that for the  $\alpha+^{90}\text{Zr}$  system. The calculated energy levels and  $B(E2)$  values obtained

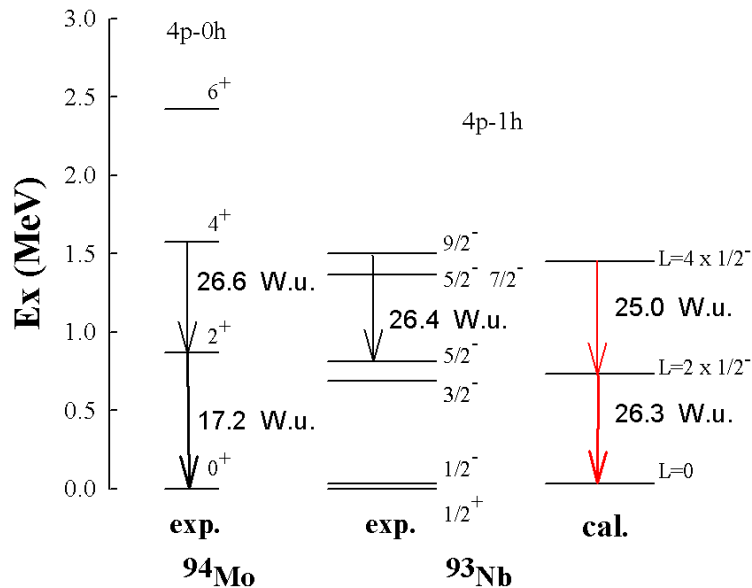


Fig. 4. (Color online) Calculated energy levels and  $B(E2)$  values of  $^{93}\text{Nb}$  are compared with the experimental data.<sup>22,23</sup> The experimental  $B(E2)$  values for  $^{94}\text{Mo}$ <sup>25</sup> are shown for comparison.

using the potential reproduce the experimental data well. The weak coupling picture due to  $\alpha$  clustering seems to persist in  $^{93}\text{Nb}$ . A systematic measurement of the  $B(E2)$  values of the nuclei in the  $^{90}\text{Zr} \sim ^{94}\text{Mo}$  region is highly desired to study the persistency of the weak coupling feature due to  $\alpha$  clustering.

### Acknowledgments

The author has been supported by a Grant-in-aid for Scientific Research of the Japan Society for Promotion of Science (No. 16540265) and the Yukawa Institute for Theoretical Physics (GCOE) where this work has been completed.

### References

1. J. Hiura and R. Tamagaki, Prog. Theor. Phys. Suppl. **52**, 25 (1972) and references therein.
2. Y. Fujiwara *et al.*, Prog. Theor. Phys. Suppl. **68**, (1980) and references therein.
3. F. Michel, S. Ohkubo, and G. Reidemeister, Prog. Theor. Phys. Suppl. **132**, 7 (1998) and references therein.
4. T. Yamaya, K. Katori, M. Fujiwara, S. Kato, and S. Ohkubo, Prog. Theor. Phys. Suppl. **132**, 73 (1998) and references therein.
5. T. Sakuda and S. Ohkubo, Prog. Theor. Phys. Suppl. **132**, 103 (1998) and references therein.
6. A. Arima, H. Horiuchi, and T. Sebe, Phys. Lett. **24B**, 129 (1967).
7. F. Nemoto and H. Bandō, Prog. Theor. Phys. **47**, 1210 (1972).
8. J. Vervier, Nucl. Phys. **75**, 17 (1966).
9. J. B. Ball and J. B. McGrory, Phys. Lett. **41B**, 581 (1972).
10. D. H. Gloeckner, Nucl. Phys. **A253**, 301 (1975).
11. S. Ohkubo, Phys. Rev. Lett. **74**, 2176 (1995).
12. B. Buck, A. C. Merchant, S. M. Perez, Phys. Rev. C **51**, 559 (1995).
13. U. Atzrott, P. Mohr, H. Abele, C. Hillenmayer, and G. Staudt, Phys. Rev. C **53**, 1336 (1996).
14. F. Michel, G. Reidemeister, and S. Ohkubo, Phys. Rev. C **61**, 041601(R) (2000).
15. M. A. Souza and H. Miyake, Brazilian J. Phys., **35**, 826 (2005).
16. G. Molnár, S. W. Yates, and R. A. Meyer, Phys. Rev. C **33**, 1843 (1986); H. Mach, G. Molnár, S. W. Yates, R. L. Gill, A. Aprahamian, and R. A. Meyer, Phys. Rev. C **37**, 254 (1988).
17. H. W. Fulbright, C. L. Bennett, R. A. Lindgren, R. G. Markham, S. C. McGuire, G. C. Morrison, U. Strohmusch, and J. Tōke, Nucl. Phys. **A284**, 329 (1977).
18. H. W. Fulbright, Phys. Rev. C **53**, 1336 (1996).
19. K. Umeda, T. Yamaya, T. Suehiro, K. Takimoto, R. Wada, E. Takada, S. Shimoura, A. Sakaguchi, S. Murakami, M. Fukada, and Y. Okuma, Nucl. Phys. **A429**, 88 (1984).
20. A. M. Van Den Berg, N. Blasi, R. H. Siemssen, and W. A. Sterrenburg, Nucl. Phys. **A403**, 57 (1983).
21. M. Wit, J. Schiele, K. A. Eberhard, and J. P. Schiffer, Phys. Rev. C **12**, 1447 (1975).
22. C. M. Baglin, Nucl. Data Sheets **80**, 1 (1997); ENSDF database (Evaluated Nuclear Structure Data File), <http://www.nndc.bnl.gov/ensdf/>.
23. J. N. Orce, C. Fransen, A. Linnemann, C. J. McKay, S. R. Leshner, N. Pietralla, V. Werner, G. Friessner, C. Kohstall, D. Mũcher, H. H. Pitz, M. Scheck,

8 *S. Ohkubo*

- C. Scholl, F. Stedile, N. Warr, S. Walter, P. von Brentano, U. Kneissl, M. T. McEllistrem, and S. W. Yates, *Phys. Rev. C* **75**, 014303 (2007).
24. G. G. Kiss, Gy Gyürky, Zs Fülöp, E. Somorjai, D. Galaviz, A. Kretschmer, K. Sonnabend, A. Zilges, P. Mohr, and M. Avrigeanu, *J. Phys. G* **35**, 014037 (2008).
25. E. Adamides, L. D. Skouras, and A. C. Xenoulis, *Phys. Rev. C* **23**, 2016 (1981).